



HAL
open science

Enhancement of Knölker Iron Catalysts for Imine Hydrogenation by Predictive Catalysis: From Calculations to Selective Experiments

Nicolas Joly, Martí Gimferrer, Sílvia Escayola, Maria Cendra, Sébastien Coufourier, Jean-François Lohier, Quentin Gaignard Gaillard, Sylvain Gaillard, Miquel Solà, Jean-Luc Renaud, et al.

► To cite this version:

Nicolas Joly, Martí Gimferrer, Sílvia Escayola, Maria Cendra, Sébastien Coufourier, et al.. Enhancement of Knölker Iron Catalysts for Imine Hydrogenation by Predictive Catalysis: From Calculations to Selective Experiments. *Organometallics*, 2023, 42 (14), pp.1784-1792. 10.1021/acs.organomet.3c00025 . hal-04222514

HAL Id: hal-04222514

<https://normandie-univ.hal.science/hal-04222514v1>

Submitted on 20 Mar 2024

HAL is a multi-disciplinary open access archive for the deposit and dissemination of scientific research documents, whether they are published or not. The documents may come from teaching and research institutions in France or abroad, or from public or private research centers.

L'archive ouverte pluridisciplinaire **HAL**, est destinée au dépôt et à la diffusion de documents scientifiques de niveau recherche, publiés ou non, émanant des établissements d'enseignement et de recherche français ou étrangers, des laboratoires publics ou privés.

Enhancement of Knölker Iron Catalysts for Imine Hydrogenation by Predictive Catalysis: From Calculations to Selective Experiments

Nicolas Joly, Martí Gimferrer, Sílvia Escayola, Maria Cendra, Sébastien Coufourier, Jean-François Lohier, Quentin Gaignard Gaillard, Sylvain Gaillard, Miquel Solà,* Jean-Luc Renaud,* and Albert Poater*



Cite This: *Organometallics* 2023, 42, 1784–1792



Read Online

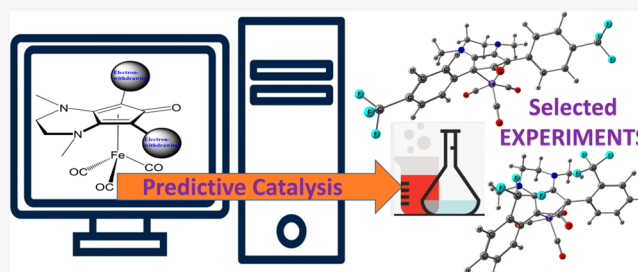
ACCESS |

Metrics & More

Article Recommendations

Supporting Information

ABSTRACT: The reductive amination reaction of imines catalyzed by Knölker-type iron complexes under hydrogen at high pressure is very interesting in synthetic terms. This type of reaction is an important catalytic challenge, since harsh conditions are necessary and do not occur easily. In a previous work (*Organometallics* 2022, 41, 1204–1215), we carried out a computational study of the reaction mechanism showing that electron-withdrawing groups (EWGs) attached to the cyclopentadienone of the Knölker-type iron complexes favor the reductive amination of imines. The synthesis of Knölker-type iron complexes with cyclopentadienones having EWGs is not straightforward, since the direct bonding of EWGs on the cyclopentadienone would lead not to the reductive amination but to undesired dimerization. A possible solution consists in the addition of phenyl substituents in the cyclopentadienones of these catalysts and then introduction of EWGs in the phenyl rings. We have performed computational studies using density functional theory (DFT) for the reductive amination of imines to analyze the efficiency of such an approach. We have found that some EWGs in the phenyl groups facilitate the reductive amination of imines. This computational result has been later confirmed experimentally, and therefore, we have computationally designed new catalysts that improve the performances of the previously known Knölker-type iron complexes.



INTRODUCTION

In the fine chemicals industry, hydrogenation plays a crucial role.¹ Although it is a very developed field of research, C=N bond hydrogenation reactions, to this day, continue to represent a challenge in the field of catalysis.² Imine-containing compounds can be obtained by condensation of an amine (primary or secondary) on a carbonyl (aldehyde or ketone). The unsaturated product obtained can then be reduced to generate an alkylated amine (secondary or tertiary). The overall pathway is then called reductive amination.³ Catalytically, efforts are mainly focused on the second part of the reductive amination process, that is the catalytic reduction of the imine into the corresponding amine, as it is a fundamental process in industry.⁴ However, many of the complexes used in homogeneous catalysis contain precious metals (or noble metals) of great economic value and resistant to corrosion, but of limited availability and with a great negative impact on the environment when extracted. Different sources of hydrogen,^{5,6} from simple molecular hydrogen⁷ to formic acid, can be used with platinum complexes.⁸ However, ruthenium became the most popular,^{9,10} owing to the outstanding Noyori^{11,12} and Shvo^{13,14} catalysts.

In recent years, economic constraints and environmental concerns have led to an increase in the demand to replace these noble metals with other more abundant metals (first

transition series) and therefore also cheaper.^{15,16} At the moment, the potential of iron as a main actor in catalysts in reductive amination processes subjected to high hydrogen pressure has been little investigated.¹⁷ From the work of Bhanage¹⁸ to the reductive amination of Beller¹⁹ and collaborators, the field has moved to milder conditions.²⁰ Another recent example is that of Renaud and collaborators, who investigated the reductive amination process of aliphatic carbonyl compounds (aldehydes and ketones) catalyzed by a Knölker complex (complex A in Scheme 1) using molecular hydrogen as a reducing agent.^{21,22} This type of catalyst is effective even with CO₂.²³ Actually, the pioneering catalyst C was synthesized in 1999 by Knölker.²⁴ With a proton donor site (ligand) and a hydride donor site (metal center),²⁵ this type of iron catalyst has a bifunctional nature, in analogy to Shvo's catalysts.

Following this line, the group of Poater and Renaud²⁶ continued to investigate the catalytic activity of the iron

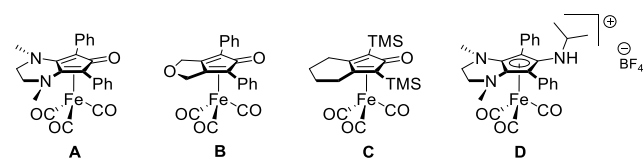
Special Issue: Advances and Applications in Catalysis with Earth-Abundant Metals

Received: January 13, 2023

Published: June 1, 2023



Scheme 1. Iron Tricarbonyl Cyclopentadienone Catalysts A–D



tricarbonyl cyclopentadienone complex C. To do this, they synthesized variants of this complex, differing in the nature of the substituents on the cyclopentadienone ring.²⁵ With the results obtained with the cyclopentadienone *N,N'*-dimethyl-3,4-ethylenediamine ligand (complex A in Scheme 1), the enhancement of the catalytic efficiency was confirmed thanks to two factors: (i) the increase of the Lewis base character of those complexes and (ii) the absence of the undesired formation of stable dimers thanks to the phenyl groups on the five-membered ring. However, despite these promising results, new improvements are still necessary in order to make these catalysts more competitive. These modifications of the complex could be based on the hypothesis that, by decreasing the electron density of the iron, its reactivity could be improved. The 2015 comparative study of the catalysts included in Scheme 1 for the reductive amination is related to the complex A owing to the *N,N'*-dimethyl-3,4-ethylenediamine ligand, complex B that demonstrates the importance of the ring annulated to the five-membered ring, and the parent Knölker catalyst C. In the case of complex A, the reaction could be carried out at 44 °C and only using 2.5 mol % complex, whereas for complexes B and C it was necessary to carry out the reaction at 85 °C and with a loading of 5 mol % to ensure a complete reductive amination, avoiding the formation of unwanted products (yields of 83, 23, and 67% for catalysts A, B, and C, respectively). In 2022, some of us proposed the modification of catalyst A. The exchange of the phenyl rings by several substituents on the cyclopentadienone was explored.²⁷ DFT calculations coupled mainly to the effective oxidation state (EOS) analysis allowed the conclusion that the presence of electron-withdrawing ligands (CF₃ and NO₂) induces a decrease of the activation energy barriers of most relevant steps, compared to the electron-donating (EDG) ligands (CH₃, OCH₃, OH, N(CH₃)₂) that worsened the kinetics. In addition, the proton transfer to the keto group of the cyclopentadienone ligand was found to be obligatorily assisted by an ethanol molecule, which induced the competition with the decarbonylation step to define the rate-determining step (rds).²⁷ The cyclopentadienone was not a spectator, but the range between nonplanarity and planarity of its five-membered ring (5-MR) was significant throughout the reaction pathway.²⁸ More importantly, electronically, the introduction of electron-withdrawing groups (EWGs) on the cyclopentadienone favors the resonance structure with 6 π electrons in the 5-MR increasing the aromaticity and the π density of this ring and decreasing the net population on the metal. These changes result in a reduction of the Fe–CO bond strength and lead to a decrease of the energy barrier of the decarbonylation step.²⁷

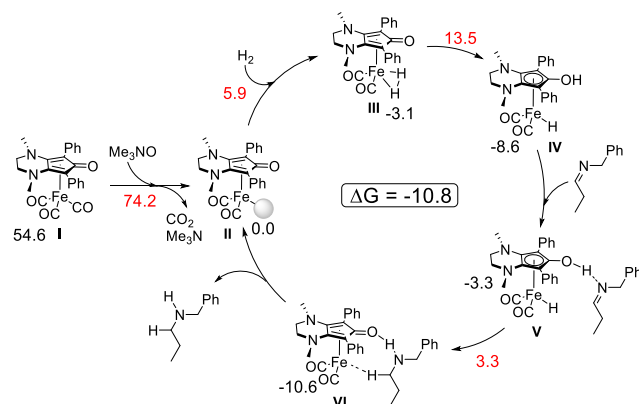
For this reason, the current study aims to improve the performance of the activity of complex A in reduction,²⁹ in terms of conversion,³⁰ to switch to milder conditions and increase the stability of the catalyst, and to avoid (or at least minimize) undesired secondary reactions. In detail, our goal is

to propose and characterize new modifications of complex A, as a predictive catalysis project, and then corroborate the obtained results experimentally. Using density functional theory (DFT) calculations, the modification of the transition metal complex A was conducted by adding different substituents on both phenyl groups of the cyclopentadienone ring. The predictive catalysis assay is performed with a selective following experimental work to increase the catalytic activity of the complex A and go beyond the yet mild conditions compared to the parent Knölker catalyst.

RESULTS AND DISCUSSION

With the use of complex A in Scheme 1 as a reference, the catalytic pathway was calculated at the M06/cc-pVTZ~SDD-(pcm-EtOH)//BP86/SVP~SDD level of theory. First, the precatalytic species I is activated with the loss of a CO ligand by oxidative elimination with trimethylamine-*N*-oxide (Me₃NO), obtaining the 16-electron intermediate II (see Scheme 2). In this first step, a CO₂ molecule is generated and

Scheme 2. General Scheme of the C=N Bond Hydrogenation for Catalyst A^a



^aRelative Gibbs energies (in kcal/mol) are given with respect to the catalytic active species II at the M06/cc-pVTZ~SDD(PCM-EtOH)//BP86/SVP~SDD (in red are the values for the transition states).²⁷

released, compensating the energy required to activate the complex with Me₃NO. This step, therefore, is favored both kinetically and thermodynamically compared to the endothermic process corresponding to the direct dissociation of the CO ligand. Next, intermediate II reacts with molecular hydrogen to generate intermediate III with H₂ η^2 -coordinated to the metal. This intermediate subsequently evolves to iron(II) hydride complex IV in which aromatization of the 5-MR facilitates the process.³¹ In this oxidation reaction, one of the hydrogen atoms has been transferred to the C=O group of the cyclopentadienone ligand. This hydrogen transfer is assisted by an explicit molecule of ethanol^{32,33} that reduces the strain on the transition state containing a 5-MR with the formation of a 7-MR. The hydroxyl group of the resulting intermediate IV can act as a Brønsted acid and activate the imine through the hydrogen bond (intermediate V). The hydrogenation of the imine forms the amine and the unsaturated iron(0) complex (II) is recovered, closing the cycle with the hydrogenation of the C=N bond of the *N*-benzyl-1-propanimine. Even though the latter could be considered as a stepwise process,^{31,34,35} this was ruled out in a former study since it is not feasible. On the

other hand, studying alternative reaction pathways, neither the product nor the substrates or solvent could better stabilize any of the intermediates when the iron center had a vacant site.²⁷ Kinetically, the last step, **V** → **VI**, is less demanding than the previous ones, and thus, for this last step, substitutions on the aryl rings on the cyclopentadienone in **Table 1** have been omitted. Actually, the most demanding step corresponds especially to two steps. The first belongs to the preactivation, **I** → **II** (19.6 kcal/mol), and the second belongs to the catalytic pathway, **III** → **IV** (16.6 kcal/mol), which increases 2.0 kcal/mol with respect to the past study,²⁷ since intermediate **III** was further stabilized by 2.0 kcal/mol.

In our first predictive catalytic study, the best catalytic candidates were those in which the phenyl rings on the cyclopentadienone rings were substituted by EWGs such as CF₃ or NO₂.²⁷ In this study, we have considered a series of other EWGs that can be experimentally more easily attached to the phenyl groups of the cyclopentadienone ligand. Even though the rds of the catalytic pathway is **III** → **IV**, the initiation step **I** → **II** was considered as well, since it could block the reaction. Different types of substituents with different substitution patterns (*ortho* (*o*-), *meta* (*m*-), and *para* (*p*-)) have been added to the phenyl rings on the cyclopentadienone complex **A**, including also EDGs for the sake of comparison. The relative Gibbs energies from **I** to **IV** are compiled in **Table S11**. How the substituents on the aryl behave or influence the metal center is not trivial, because when the hydrogenated aryl rings are replaced by perfluorinated ones, the two kinetically demanding energy barriers increase by 0.6 kcal/mol. However, this result could be linked not only to electronic effects on the metal center but also to H-bond formation with the fluorides. Results must be read in detail, and the analysis of the different substituents on the cyclopentadienone becomes complicated when there is the aryl in between. Centering first on the species with just a substituent in *para*, to exclude any interaction with the metal center, and the noncovalent interactions, the energy barrier for **III** → **IV** goes up by 0.9, 3.5, and 0.6 kcal/mol for NO₂, NMe₂, and COOEt phenyl substituted rings as compared to the unsubstituted case, respectively, whereas it goes down by 0.4, 1.4, and 2.0 kcal/mol for substituents OMe, CF₃, and COOMe, respectively. No clear trend among EWGs and EDGs is extracted, but the EDG NMe₂ clearly has a worse performance. In addition, the initiation is clearly disfavored for all the EDGs by at least 0.2 kcal/mol, with values ranging from 19.8 to 24.8 kcal/mol. Another clear point is that the substitution in *ortho* does not favor any of the limiting transition states, and the combination of *ortho* with *para* substitution reinforces this conclusion, whereas interestingly in *meta* the interaction is clearly favored for OMe and CF₃.

As said before, the presence of an EWG in the cyclopentadienone ligand makes the Fe–C(O) bonds more labile; thus the catalyst can enter the catalytic cycle faster. Substitution of the aryl rings on the cyclopentadienone, instead of direct substitution on the cyclopentadienone ring, makes the analysis more complicated. However, results in **Table 1** show that the addition of EDGs confirms the trend of worsening catalytic performance, since the corresponding energy barriers are significantly higher, especially for the **I** → **II** decarbonylation step (consider, for instance, the cases Ph(*p*-NMe₂), Ph(*o*-OMe), Ph(*o*-,*o*-OMe), and Ph(*o*-,*o*-*p*-OMe)).

We have also analyzed the performance of cationic catalyst **D** (**Scheme 1**), where instead of having the keto group in the cyclopentadienone we have an *N*-methyl cationic group, whose

Table 1. Relevant Gibbs Energy Barriers of Steps **I–II** and **III–IV** Obtained at the M06/cc-pVTZ~SDD(PCM-EtOH)//BP86/SVP~SDD level (in kcal/mol) for the Differently Substituted Catalysts **A**, Substituting Both Aryl Rings (Ph) on the Cyclopentadienone by a Series of Other Aryl Rings^a

	Ph	C ₆ F ₅	Ph(<i>p</i> -NO ₂)	Ph(<i>p</i> -NMe ₂)	Ph(<i>o</i> -OMe)	Ph(<i>m</i> -OMe)	Ph(<i>p</i> -OMe)	Ph(<i>o</i> -CF ₃)	Ph(<i>m</i> -CF ₃)	Ph(<i>p</i> -CF ₃)	Ph(<i>p</i> -COOMe)	Ph(<i>p</i> -COOEt)	Ph(<i>o</i> -, <i>o</i> -OMe)	Ph(<i>o</i> -, <i>o</i> -OMe)	Ph(<i>o</i> -, <i>o</i> - <i>p</i> -OMe)	Ph(<i>o</i> -, <i>o</i> -CF ₃)	Ph(<i>o</i> -, <i>o</i> - <i>p</i> -CF ₃)
Δ <i>G</i> (I–II)	19.6	20.2	19.8	24.8	22.1	20.3	19.8	18.7	15.7	18.7	15.2	13.5	25.6	26.2	19.1	16.2	
Δ <i>G</i> (III–IV) ^b	16.6	17.2	17.5	20.1	18.4	15.3	16.2	15.2	15.5	15.2	14.6	17.2	19.3	18.5	21.3	22.0	

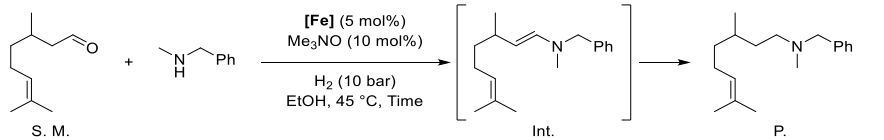
^aMe = methyl, Et = ethyl, Ph = phenyl. ^bProton transfer assisted by one ethanol molecule.

Table 2. Relevant Gibbs Energy Barriers of Steps I–II and III–IV Obtained at the M06/cc-pVTZ~SDD(PCM-EtOH)//BP86/SVP~SDD level (in kcal/mol) for the Differently Substituted Catalyst D, Where the Amino Group Is NMe⁺ and When Adding the BF₄[−] Counteranion^a

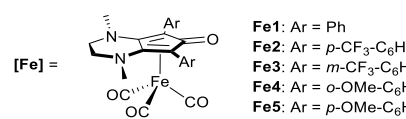
	Ph	Ph(<i>p</i> -CF ₃)	Ph(<i>o</i> -OMe)	Ph (BF ₄ [−])	Ph(<i>p</i> -CF ₃)(BF ₄ [−])	Ph(<i>o</i> -OMe)(BF ₄ [−])
ΔG(I–II)	13.4	10.6	14.2	16.4	14.4	17.1
ΔG(III–IV) ^b	20.1	19.8	22.1	23.2	23.5	22.3

^aMe = methyl, Ph = phenyl. ^bProton transfer assisted by one ethanol molecule.

Table 3. Selectivities Obtained for the Reductive Amination, Starting Material/Intermediate/Product (S.M./Int./P.), Using Catalyst A (Fe1) and Its Modified Forms with CF₃ and OMe Groups in *ortho*, *meta* and *para* Positions of the Phenyls^a



[Fe] =



- Fe1: Ar = Ph
- Fe2: Ar = *p*-CF₃-C₆H₅
- Fe3: Ar = *m*-CF₃-C₆H₅
- Fe4: Ar = *o*-OMe-C₆H₅
- Fe5: Ar = *p*-OMe-C₆H₅

time (h)	Fe1	Fe2	Fe3	Fe4	Fe5
1	24/17/5	32/36/5	47/47/4	56/44/0	75/25/0
2	9/73/18	18/47/35	35/40/25	43/57/0	48/47/5
5	27/38/36	0/0/100	0/0/100	0/100/0	8/70/22

^aGeneral conditions: citronellal (1 mmol), *N*-methylbenzylamine (2 mmol), [Fe] (5 mol %), Me₃NO (10 mol %), ethanol (2 mL), H₂ (10 bar), 45 °C.

positive charge would be compensated by a BF₄[−] group. Although in previous studies the role of the counterion was not found to be indispensable,³⁶ except for a recent work by Bütikofer and Chen,³⁷ here we have quantified the effect of the counterion. Table 2 and Table S11 contain the comparative results. Without BF₄[−], and as previously seen, this is a catalyst that would be worse for reductive amination (by 3.5 kcal/mol), but not so for activation, which would become 6.2 kcal/mol more favorable (comparing the two systems with only simple nonsubstituted phenyls on the cyclopentadienone in Table 2, with further details in Table S12). However, we attempted to overcome the worsening catalytic barrier by introducing *o*-CF₃ substituents in the Ph groups, albeit with only an improvement of 0.3 kcal/mol for step III → IV, and interestingly 2.8 kcal/mol for step I → II. For comparison, the methoxy substitution led to an increase in the two barriers, specifically by 0.8 and 2.0 kcal/mol, respectively. Including the counterion BF₄[−], the results were qualitatively identical, but with an approximate 2–3 kcal/mol increase of the two barriers. Although these calculations might seem sterile, the trends allow corroboration of the results of catalyst A showing that by adding CF₃ groups in *para* positions the catalytic efficiency improves (compare Ph and Ph(*p*-CF₃)). Ph(*p*-CF₃) is the ideal system for predictive catalysis research, because from an experimental point of view Ph(*p*-CF₃) is easily achieved in the lab (*vide infra*).

Steric maps by the SambVca2.1 package³⁸ were carried out to see how they affect the groups located in the cyclopentadienone, specifically the phenyls *ortho* to the keto group, as well as the *para* substitution thereof. However, Figure S38 confirms, with the steric maps and percent buried volume (% V_{Bur}), that no significant difference is observed for the systems. More interestingly, the systems studied in the previous computational work,²⁷ where substituents were bonded directly to the cyclopentadienone, generated no difference in steric hindrance. Actually, with CF₃ directly bonded to the cyclopentadienone ring, a %V_{Bur} even 0.3% higher was shown. Thus, structurally the differences between the different species are scarce, and actually, the analyses of the bond distances or Mayer bond orders (MBOs) confirm this (see Tables S5 and

S6).³⁹ Electronically, we analyzed the NPA charges (Table S7) on the iron center for a selection of systems,⁴⁰ observing that when the catalyst contains EWG substituents the metal partial charge is lower (gives electron density to the ligand), but not significantly.

We again confirmed that the role of the cyclopentadienone ligand in the catalytic performance of the systems cannot be rationalized in terms of aromaticity changes depending on its substituents.⁴¹ The results are collected in Tables S8 and S9, together with their discussion in the Supporting Information.⁴² Briefly, for the six-membered ring attached to the cyclopentadienone, as expected, no drastic change is observed, since the phenyls are not attached directly to the metal. Actually, this six-membered ring between the cyclopentadienone and the different substituents is not relevant.⁴³ Nevertheless, a simple means of transport for the electron density gain or loss on the metal center is generated by those different substituents.

To understand the different nature of the first two intermediates, we applied EOS analysis (see technical details in the Supporting Information).^{44,45} The results obtained for different degrees of substitution of the two phenyls attached to the cyclopentadienone are collected in Table S10. The frontier effective fragment orbitals (EFOs) are for the metal (last occupied (LO) with a pair of electrons assigned) versus the cyclopentadienone ligand (first unoccupied (FU)). Only for Ph(*o*-OMe) does this differ, where the FU EFO corresponds to the metal, too. With this, both the metal and cyclopentadienone ligand present the expected neutral (0) oxidation state. Overall, small differences are observed between the values of the reliability index (*R* (%)) in both species (±3% versus Ph), being greater for species II (*R* (%) > 65) than for I (50 < *R* (%) < 60).

The π-acid character from the CO units can be assessed by comparing the appropriate EFO occupations between species I and II. CO as a π-acid agent has the ability to remove density from the metal. By removing a CO, the metal center becomes slightly more negative. This is validated by the increase of occupation of the LO EFO (d-type from metal, Table S10).

The largest differences are found with C_6F_6 , $Ph(o-CF_3)$, and $Ph(o-OMe)$.

Finally, and making practical use of predictive catalysis, it was proposed to confirm the previous computational results with experiments. Although the best system was predicted to be with methyl ester substituents in the *para* positions of the phenyls, for synthetic reasons we focused on four derivatives of complex **A**, complexes **Fe2**, **Fe3**, **Fe4**, and **Fe5**, bearing *p*- CF_3 , *m*- CF_3 , *o*-OMe, and *p*-OMe, respectively. These complexes were prepared following the same procedure used for **Fe1** (complex **A**). Even though not all modifications become favorable on the cyclopentadienone moiety,⁴⁶ the predicted results from the DFT calculations could be translated into experiments. The conversions and selectivities obtained for the original complex **A** and its derived **Fe2**–**Fe5** are summarized in Table 3. With the modification of the phenyls, incorporating the CF_3 group in a *para* (**Fe2**) or *meta* (**Fe3**) position, a considerable improvement of the reaction was achieved. In addition, over time, specifically after 5 h, a total conversion into the desired product (**P**) was obtained (versus 36% for **Fe1**), working only at 45 °C. On the contrary, the results for the reductive amination with complexes **Fe4** and **Fe5** follow the trend previously observed for EDG-substituted catalysts. OMe-substituted phenyls of the cyclopentadienone ligand worsen the activity of the complex. Perhaps, it is also important to consider that, in the case of complex **Fe4**, the total absence of conversion into the alkylated amine can also be explained by the *ortho* substitution which could sterically hinder the active site of the iron atom and consequently block the approach of the substrates (see the Supporting Information for further details).

The latest results open the door to the design of a new series of catalysts based on introducing modifications to the phenyl groups in order to improve their activity by modulating steric and/or electronic effects. More research is underway to computationally test new complexes with different substituents on the phenyls of the cyclopentadienone. We want to study the energy changes in the reaction mechanism of the catalytic cycle and also rationalize these changes based on the electronic and steric effects present in each case. In this way, we hope to improve the rational design of Knölker catalysts for reductive amination of imines with more favorable activation barriers.⁴⁷

CONCLUSIONS

In the search for more efficient iron derivative Knölker catalysts to conduct the reductive amination of imines, we decided to use the results of a previous computational study, where it was predicted that reductive amination reactions would be especially favored by substituting phenyls by electron-withdrawing groups, especially trifluoromethyl groups. Because the synthesis of substituted cyclopentadienones was not experimentally feasible, we decided to analyze the same complex but substituting the phenyl groups of the cyclopentadienone instead of the cyclopentadienone itself.

Results show that the energy barriers vary relatively little for the different electron-withdrawing and electron-donating substituents and without a clear trend, but there is the exception of the CF_3 group in a *para* position for the phenyls of the cyclopentadienone, where a better result is obtained regarding the catalyst activation. In particular, DFT calculations show that the energy barrier of the rds decreases by 0.9 kcal/mol, which is not as significant as it would be if we put the EWG directly on the cyclopentadienone, but the trend

between the different substituent groups on the two aryl groups of the cyclopentadienone confirms the validity of the DFT results, even if they show relatively small differences for the different substitutions. The effect is almost purely electronic as structural measures and steric maps prove that the substituents of the cyclopentadienone do not affect the catalytic activity at all, since they are relatively far from the iron. Next, the synthesis of the catalysts was achieved experimentally and we found that the catalytic activity increased significantly, turning what might seem like a computational entelechy into an experimental reality, making real use of predictive catalysis. Simply, the experiments become here a general observation to confirm the trend observed by DFT.

COMPUTATIONAL DETAILS

All calculations were conducted at the DFT level with the Gaussian 09 set of programs,⁴⁸ using the BP86 functional.⁴⁹ The electronic configuration of the molecular systems was described with the standard split-valence basis set with a polarization function of Ahlrichs and co-workers for H, C, N, O, and F (SVP keyword in Gaussian).⁵⁰ For Fe, the quasi-relativistic Stuttgart/Dresden effective core potential⁵¹ with an associated valence basis set (standard SDD keyword in Gaussian 09) was used. Geometry optimizations were carried out without symmetry constraints, and normal-mode analyses were computed to confirm minima and transition states on the potential energy surface. These frequencies were used to calculate unscaled zero-point energies (ZPEs) as well as thermal corrections and entropy effects at 298 K and 1 atm by using the standard statistical mechanics relationships for an ideal gas. Accurate electronic energies were obtained via single-point calculation using the M06 functional of Zhao and Truhlar,⁵² on the BP86-optimized geometries. In these calculations, the cc-pVTZ basis set was used for the descriptions of H, C, N, O, and F,⁵³ whereas for Fe the SDD basis set (and pseudopotential) has been employed, together with the solvent effects of ethanol estimated with the polarizable continuous solvation model (PCM).^{54,55} On top of the M06/cc-pVTZ~SDD(PCM-EtOH) electronic energies, we added the thermal and entropy corrections obtained at the BP86/SVP~SDD level in the gas phase.

ASSOCIATED CONTENT

Supporting Information

The Supporting Information is available free of charge at <https://pubs.acs.org/doi/10.1021/acs.organomet.3c00025>.

Experimental and spectroscopic details of the catalytic reactions; absolute energies of all studied systems; additional discussion on steric maps, aromaticity and effective oxidation states (PDF)

XYZ coordinates of studied systems (XYZ)

Accession Codes

CCDC 2247199–2247202 contain the supplementary crystallographic data for this paper. These data can be obtained free of charge via www.ccdc.cam.ac.uk/data_request/cif, or by emailing data_request@ccdc.cam.ac.uk, or by contacting The Cambridge Crystallographic Data Centre, 12 Union Road, Cambridge CB2 1EZ, UK; fax: +44 1223 336033.

AUTHOR INFORMATION

Corresponding Authors

Miquel Solà – Institut de Química Computacional i Catàlisi and Departament de Química, Universitat de Girona, 17003 Girona, Catalonia, Spain; orcid.org/0000-0002-1917-7450; Email: miquel.sola@udg.edu

Jean-Luc Renaud – Normandie Université, LCMT, ENSICAEN, UNICAEN, CNRS, 14000 Caen, France; orcid.org/0000-0001-8757-9622; Email: jean-luc.renaud@ensicaen.fr

Albert Poater – Institut de Química Computacional i Catàlisi and Departament de Química, Universitat de Girona, 17003 Girona, Catalonia, Spain; orcid.org/0000-0002-8997-2599; Email: albert.poater@udg.edu

Authors

Nicolas Joly – Institut de Química Computacional i Catàlisi and Departament de Química, Universitat de Girona, 17003 Girona, Catalonia, Spain; Normandie Université, LCMT, ENSICAEN, UNICAEN, CNRS, 14000 Caen, France

Martí Gimferrer – Institut de Química Computacional i Catàlisi and Departament de Química, Universitat de Girona, 17003 Girona, Catalonia, Spain; orcid.org/0000-0001-5222-2201

Silvia Escayola – Institut de Química Computacional i Catàlisi and Departament de Química, Universitat de Girona, 17003 Girona, Catalonia, Spain; Donostia International Physics Center (DIPC), 20018 Donostia, Euskadi, Spain; orcid.org/0000-0002-1159-7397

Maria Cendra – Institut de Química Computacional i Catàlisi and Departament de Química, Universitat de Girona, 17003 Girona, Catalonia, Spain

Sébastien Coufourier – Normandie Université, LCMT, ENSICAEN, UNICAEN, CNRS, 14000 Caen, France; orcid.org/0000-0002-6432-6144

Jean-François Lohier – Normandie Université, LCMT, ENSICAEN, UNICAEN, CNRS, 14000 Caen, France

Quentin Gaignard Gaillard – Normandie Université, LCMT, ENSICAEN, UNICAEN, CNRS, 14000 Caen, France

Sylvain Gaillard – Normandie Université, LCMT, ENSICAEN, UNICAEN, CNRS, 14000 Caen, France; orcid.org/0000-0003-3402-2518

Complete contact information is available at:

<https://pubs.acs.org/10.1021/acs.organomet.3c00025>

Author Contributions

All authors have given approval to the final version of the manuscript.

Notes

The authors declare no competing financial interest.

ACKNOWLEDGMENTS

S.G., N.J., and J.-L.R. gratefully acknowledge financial support from the “Ministère de la Recherche et des Nouvelles Technologies”, Normandie Université, CNRS, and the LABEX SynOrg (ANR-11-LABX-0029). N.J. acknowledges the Graduate School of Research XL-Chem (ANR-18-EURE0020 XL-Chem) for the PhD fellowship. A.P. and M.S. are grateful for financial support from the Ministerio de Ciencia e Innovación (PID2021-127423NB-I00, PGC2018-098212-B-C22, and PID2020-13711GB-I00) and Generalitat de Catalunya for Project 2021SGR623 and ICREA Academia

prize 2019. A.P. is a Serra Hùnter fellow. M.G. thanks the Generalitat de Catalunya and Fons Social Europeu for a predoctoral fellowship (2018 FI_B01120). S.E. thanks Universitat de Girona and Donostia International Physics Center (DIPC) for an IFUDG2019 predoctoral fellowship. The authors thank Dr. Pedro Salvador for insightful comments.

REFERENCES

- (1) Parshall, G. W.; Steven, D. I. In *Homogeneous Catalysis. The Applications and Chemistry of Catalysis by Soluble Transition Metal Complexes*; Wiley: New York, 1992; pp 25–50.
- (2) (a) El-Sepelgy, O.; Alandini, N.; Rueping, M. Merging Iron Catalysis and Biocatalysis—Iron Carbonyl Complexes as Efficient Hydrogen Autotransfer Catalysts in Dynamic Kinetic Resolutions. *Angew. Chem., Int. Ed.* **2016**, *55*, 13602–13605. (b) El-Sepelgy, O.; Brzozowska, A.; Azofra, L. M.; Jang, Y. K.; Cavallo, L.; Rueping, M. Experimental and Computational Study of an Unexpected Iron-Catalyzed Carboetherification by Cooperative Metal and Ligand Substrate Interaction and Proton Shuttling. *Angew. Chem., Int. Ed.* **2017**, *56*, 14863–14867.
- (3) Nugent, T. C.; Ghosh, A. K.; Wakchaure, V. N.; Mohanty, R. R. Asymmetric Reductive Amination: Convenient Access to Enantioenriched Alkyl-Alkyl or Aryl-Alkyl Substituted α -Chiral Primary Amines. *Adv. Synth. Catal.* **2006**, *348*, 1289–1299.
- (4) Piontek, A.; Bisz, E.; Szostak, M. Iron-Catalyzed Cross-Couplings in the Synthesis of Pharmaceuticals: In Pursuit of Sustainability. *Angew. Chem., Int. Ed.* **2018**, *57*, 11116–11128.
- (5) For selected reviews: (a) Bahn, S.; Imm, S.; Neubert, L.; Zhang, M.; Neumann, H.; Beller, M. The Catalytic Amination of Alcohols. *ChemCatChem* **2011**, *3*, 1853–1864. (b) Yang, Q.; Wang, Q.; Yu, Z. Substitution of Alcohols by N-Nucleophiles via Transition Metal-Catalyzed Dehydrogenation. *Chem. Soc. Rev.* **2015**, *44*, 2305–2329. (c) Renaud, J.-L.; Gaillard, S. Recent Advances in Iron- and Cobalt-Complex-Catalyzed Tandem/Consecutive Processes Involving Hydrogenation. *Synthesis* **2016**, *48*, 3659–3683. (d) Quintard, A.; Rodriguez, J. A Step into an eco-Compatible Future: Iron- and Cobalt-catalyzed Borrowing Hydrogen Transformation. *ChemSusChem* **2016**, *9*, 28–30.
- (6) For some recent articles on iron complexes-catalyzed amine alkylation: (a) Yan, T.; Feringa, B. L.; Barta, K. Iron Catalyzed Direct Alkylation of Amines with Alcohols. *Nat. Commun.* **2014**, *5*, 5602–5609. (b) Yan, T.; Feringa, B. L.; Barta, K. Benzylamines via Iron-Catalyzed Direct Amination of Benzyl Alcohols. *ACS Catal.* **2016**, *6*, 381–388. (c) Yan, T.; Feringa, B. L.; Barta, K. Direct N-alkylation of unprotected amino acids with alcohols. *Sci. Adv.* **2017**, *3*, No. ea06494. (d) Mastalir, M.; Stöger, B.; Pittenauer, E.; Allmaier, G.; Kirchner, G.; Puchberger, M. Air Stable Iron(II) PNP Pincer Complexes as Efficient Catalysts for the Selective Alkylation of Amines with Alcohols. *Adv. Synth. Catal.* **2016**, *358*, 3824–3831. (e) Brown, T. J.; Cumbes, M.; Diorazio, L. J.; Clarkson, G. J.; Wills, M. Use of (Cyclopentadienone)iron Tricarbonyl Complexes for C–N Bond Formation Reactions between Amines and Alcohols. *J. Org. Chem.* **2017**, *82*, 10489–10503. (f) Pan, H.-J.; Ng, T. W.; Zhao, Y. Iron-Catalyzed Amination of Alcohols Assisted by Lewis Acid. *Chem. Commun.* **2015**, *51*, 11907–11910. (g) Polidano, K.; Allen, B. D. W.; Williams, J. M. J.; Morrill, L. C. Iron-Catalyzed Methylation Using the Borrowing Hydrogen Approach. *ACS Catal.* **2018**, *8*, 6440–6445. (h) Bettoni, L.; Joly, N.; Lohier, J.-F.; Gaillard, S.; Poater, A.; Renaud, J.-L. Ruthenium-Catalyzed Three-Component Alkylation: A Tandem Approach to the Synthesis of Nonsymmetric *N,N*-Dialkyl Acyl Hydrazides with Alcohols. *Adv. Synth. Catal.* **2021**, *363*, 4009–4017. (i) Abdallah, M.-S.; Joly, N.; Gaillard, S.; Poater, A.; Renaud, J.-L. Blue-Light Induced Iron-Catalyzed α -Alkylation of Ketone. *Org. Lett.* **2022**, *24*, 5584–5589. (j) Lator, A.; Gaillard, Q. G.; Mérel, D. S.; Lohier, J.-F.; Gaillard, S.; Poater, A.; Renaud, J.-L. Room-Temperature Chemoselective Reductive Alkylation of Amines Catalyzed by a Well-Defined Iron(II) Complex Using Hydrogen. *J. Org. Chem.* **2019**, *84*, 6813–6829. (k) Emayavarambala, B.; Chakraborty, P.; Dahiya, P.;

Sundararaju, B. Iron-Catalyzed α -Methylation of Ketones Using Methanol as the C1 Source under Photoirradiation. *Org. Lett.* **2022**, *24*, 6219–6223.

(7) For some examples, see: (a) Ikenaga, T.; Matsushita, K.; Shinozawa, J.; Yada, S.; Takagi, Y. The Effects of Added Ammonium Chloride in The Reductive Amination of Some Carbonyl Compounds over Ru and Pd Catalysts. *Tetrahedron* **2005**, *61*, 2105–2109. (b) Falus, P.; Boros, Z.; Hornyanszky, G.; Nagy, J.; Darvas, F.; Ürge, L.; Poppe, L. Reductive Amination of Ketones: Novel One-Step Transfer Hydrogenations in Batch and Continuous-Flow Mode. *Tetrahedron Lett.* **2011**, *52*, 1310–1312. (c) Wei, D.; Bruneau-Voisine, A.; Valyaev, D. A.; Lugan, N.; Sortais, J.-B. Manganese catalyzed reductive amination of aldehydes using hydrogen as a reductant. *Chem. Commun.* **2018**, *54*, 4302–4305. and references cited therein.

(8) For some recent examples, see: (a) Wang, C.; Pettman, A.; Basca, J.; Xiao, J. A Versatile Catalyst for Reductive Amination by Transfer Hydrogenation. *Angew. Chem., Int. Ed.* **2010**, *49*, 7548–7552. (b) Huang, Y.-B.; Dai, J.-J.; Deng, X.-J.; Qu, Y.-C.; Guo, Q.-X.; Fu, Y. Ruthenium-Catalyzed Conversion of Levulinic Acid to Pyrrolidines by Reductive Amination. *ChemSusChem* **2011**, *4*, 1578–1581. (c) Wang, S.; Huang, H.; Bruneau, C.; Fischmeister, C. Selective and Efficient Iridium Catalyst for the Reductive Amination of Levulinic Acid into Pyrrolidones. *ChemSusChem* **2017**, *10*, 4150–4154. (d) Wei, Y.; Wang, C.; Jiang, X.; Xue, D.; Li, J.; Xiao, J. Highly Efficient Transformation of Levulinic Acid into Pyrrolidinones by Iridium Catalyzed Transfer Hydrogenation. *Chem. Commun.* **2013**, *49*, 5408–5410. (e) Zhu, M. Ruthenium-Catalyzed Direct Reductive Amination in HCOOH/NEt₃ Mixture. *Catal. Lett.* **2014**, *144*, 1568–1572. (f) Yang, P.; Lim, L. H.; Chuanprasit, P.; Hirao, H.; Zhou, J. S. Nickel-Catalyzed Enantioselective Reductive Amination of Ketones with Both Arylamines and Benzhydrazide. *Angew. Chem., Int. Ed.* **2016**, *55*, 12083–12087. (g) Metzker, G.; Dias, R. M. P.; Burtoloso, A. C. B. Iron-Catalyzed Reductive Amination from Levulinic and Formic Acid Aqueous Solutions: An Approach for the Selective Production of Pyrrolidones in Biorefinery Facilities. *ChemistrySelect* **2018**, *3*, 368–372.

(9) Zhou, Q.-L.; Xie, J.-H. Transition metal-catalyzed enantioselective hydrogenation of enamides and enamines. *Top. Curr. Chem.* **2013**, *343*, 75–101.

(10) (a) Privalov, T.; Samec, J. S. M.; Bäckvall, J.-E. DFT Study of an Inner-Sphere Mechanism in the Hydrogen Transfer from a Hydroxycyclopentadienyl Ruthenium Hydride to Imines. *Organometallics* **2007**, *26*, 2840–2848. (b) Comas-Vives, A.; Ujaque, G.; Lledós, A. Hydrogen Transfer to Ketones Catalyzed by Shvo's Ruthenium Hydride Complex: A Mechanistic Insight. *Organometallics* **2007**, *26*, 4135–4144. (c) Comas-Vives, A.; Ujaque, G.; Lledós, A. Theoretical Analysis of the Hydrogen-Transfer Reaction to C=N, C=C, and C≡C Bonds Catalyzed by Shvo's Ruthenium Complex. *Organometallics* **2008**, *27*, 4854–4863.

(11) (a) Noyori, R.; Umeda, I.; Ishigami, T. Selective hydrogenation of α,β -unsaturated carbonyl compounds via hydridoiron complexes. *J. Org. Chem.* **1972**, *37*, 1542–1545. (b) Lee, H.-Y.; An, M. Selective 1,4-reduction of unsaturated carbonyl compounds using Co₂(CO)₈-H₂O. *Tetrahedron Lett.* **2003**, *44*, 2775–2778.

(12) (a) Ikariya, T.; Murata, K.; Noyori, R. Bifunctional Transition Metal-Based Molecular Catalysts for Asymmetric Syntheses. *Org. Biomol. Chem.* **2006**, *4*, 393–406. (b) Muñiz, K. Bifunctional Metal-Ligand Catalysis: Hydrogenations and New Reactions Within the Metal-(Di)amine Scaffold. *Angew. Chem., Int. Ed.* **2005**, *44*, 6622–6627. (c) Ikariya, T. Chemistry of Concerto Molecular Catalysis Based on the Metal/NH Bifunctionality. *Bull. Chem. Soc. Jpn.* **2011**, *84*, 1–16. (d) Ito, M.; Ikariya, T. Catalytic Hydrogenation of Polar Organic Functionalities Based on Ru-Mediated Heterolytic Dihydrogen Cleavage. *Chem. Commun.* **2007**, 5134–5142.

(13) Shvo, Y.; Czarkie, D.; Rahamim, Y.; Chodosh, D. F. A new group of ruthenium complexes: structure and catalysis. *J. Am. Chem. Soc.* **1986**, *108*, 7400–7402.

(14) Blum, Y.; Czarkie, D.; Rahamim, Y.; Shvo, Y. (Cyclopentadienone)ruthenium Carbonyl Complexes - A New Class of Homogeneous Hydrogenation Catalysts. *Organometallics* **1985**, *4*, 1459–1461.

(15) (a) Elangovan, S.; Topf, C.; Fischer, S.; Jiao, H.; Spannenberg, A.; Baumann, W.; Ludwig, R.; Junge, K.; Beller, M. Selective Catalytic Hydrogenations of Nitriles, Ketones, and Aldehydes by Well-Defined Manganese Pincer Complexes. *J. Am. Chem. Soc.* **2016**, *138*, 8809–8814. (b) Rösler, S.; Obenauf, J.; Kempe, R. A Highly Active and Easily Accessible Cobalt Catalyst for Selective Hydrogenation of C=C O Bonds. *J. Am. Chem. Soc.* **2015**, *137*, 7998–8001.

(16) (a) Bauer, I.; Knölker, H.-J. Iron Catalysis in Organic Synthesis. *Chem. Rev.* **2015**, *115*, 3170–3387. (b) Gopalaiah, K. Chiral Iron Catalysts for Asymmetric Synthesis. *Chem. Rev.* **2013**, *113*, 3248–3296. (c) Bullock, R. M. Abundant Metals Give Precious Hydrogenation Performance. *Science* **2013**, *342*, 1054–1055. (d) Mérel, D. S.; Do, M. L. D.; Gaillard, S.; Dupau, P.; Renaud, J.-L. Iron-catalyzed reduction of carboxylic and carbonic acid derivatives. *Coord. Chem. Rev.* **2015**, *288*, 50–68. (e) Dupau, P.; Tran Do, M. L.; Gaillard, S.; Renaud, J.-L. Iron-Catalyzed Hydrogenation of Esters to Alcohols. *Angew. Chem., Int. Ed.* **2014**, *53*, 13004–13006. (f) Sues, P. E.; Demmans, K. Z.; Morris, R. H. Rational development of iron catalysts for asymmetric transfer hydrogenation. *Dalton Trans.* **2014**, *43*, 7650–7667. (g) Greenhalgh, M. D.; Jones, A. S.; Thomas, S. P. Iron-Catalysed Hydrofunctionalisation of Alkenes and Alkynes. *ChemCatChem* **2015**, *7*, 190–222. (h) Zell, T.; Milstein, D. Hydrogenation and Dehydrogenation Iron Pincer Catalysts Capable of Metal-Ligand Cooperation by Aromatization/De aromatization. *Acc. Chem. Res.* **2015**, *48*, 1979–1994. (i) Morris, R. H. Exploiting Metal-Ligand Bifunctional Reactions in the Design of Iron Asymmetric Hydrogenation Catalysts. *Acc. Chem. Res.* **2015**, *48*, 1494–1502. (j) Misal Castro, L. C.; Li, H.; Sortais, J.-B.; Darcel, C. When iron met phosphines: a happy marriage for reduction catalysis. *Green Chem.* **2015**, *17*, 2283–2303. (k) Bigler, R.; Huber, R.; Mezzetti, A. Iron Chemistry Made Easy: Chiral N₂P₂ Ligands for Asymmetric Catalysis. *Synlett* **2016**, *27*, 831–847. (l) McNeill, E.; Ritter, T. 1,4-Functionalization of 1,3-Dienes With Low-Valent Iron Catalysts. *Acc. Chem. Res.* **2015**, *48*, 2330–2343.

(17) (a) Liu, J.; Song, Y.; Ma, L. Earth-abundant Metal-catalyzed Reductive Amination: Recent Advances and Prospect for Future Catalysis. *Chem.—Asian J.* **2021**, *16*, 2371–2391. (b) Irrgang, T.; Kempe, R. Transition-metal-catalyzed reductive amination employing hydrogen. *Chem. Rev.* **2020**, *120*, 9583–9674.

(18) Bhor, M. D.; Bhanushali, M. J.; Nandurkar, N. S.; Bhanage, B. M. Direct reductive amination of carbonyl compounds with primary/secondary amines using recyclable water-soluble Fe^{II}/EDTA complex as catalyst. *Tetrahedron Lett.* **2008**, *49*, 965–969.

(19) Fleischer, S.; Zhou, S.; Junge, K.; Beller, M. An Easy and General Iron-catalyzed Reductive Amination of Aldehydes and Ketones with Anilines. *Chem.—Asian J.* **2011**, *6*, 2240–2245.

(20) (a) Fleischer, S.; Zhou, S.; Junge, K.; Beller, M. General and Highly Efficient Iron-Catalyzed Hydrogenation of Aldehydes, Ketones, and α,β -Unsaturated Aldehydes. *Angew. Chem., Int. Ed.* **2013**, *52*, 5120–5124. (b) Gorgas, N.; Stöger, B.; Veiros, L. F.; Kirchner, K. Highly Efficient and Selective Hydrogenation of Aldehydes: A Well-Defined Fe(II) Catalyst Exhibits Noble-Metal Activity. *ACS Catal.* **2016**, *6*, 2664–2672. (c) Mazza, S.; Scopelliti, R.; Hu, X. Chemoselective Hydrogenation and Transfer Hydrogenation of Aldehydes Catalyzed by Iron(II) PONOP Pincer Complexes. *Organometallics* **2015**, *34*, 1538–1545. (d) Wienhöfer, G.; Westerhaus, F. A.; Junge, K.; Ludwig, R.; Beller, M. A Molecularly Defined Iron-Catalyst for the Selective Hydrogenation of α,β -Unsaturated Aldehydes. *Chem.—Eur. J.* **2013**, *19*, 7701–7707.

(21) Thai, T.-T.; Mérel, D. S.; Poater, A.; Gaillard, S.; Renaud, J.-L. Highly Active Phosphine-Free Bifunctional Iron Complex for Hydrogenation of Bicarbonate and Reductive Amination. *Chem.—Eur. J.* **2015**, *21*, 7066–7070.

- (22) Lator, A.; Gaillard, S.; Poater, A.; Renaud, J.-L. Iron-Catalyzed Chemoselective Reduction of α,β -Unsaturated Ketones. *Chem.—Eur. J.* **2018**, *24*, 5770–5774.
- (23) (a) Coufourier, S.; Gagnard-Gaillard, Q.; Lohier, J.-F.; Poater, A.; Gaillard, S.; Renaud, J.-L. Hydrogenation of CO₂, Hydrogenocarbonate, and Carbonate to Formate in Water using Phosphine Free Bifunctional Iron Complexes. *ACS Catal.* **2020**, *10*, 2108–2116. (b) Coufourier, S.; Gaillard, S.; Clet, G.; Serre, C.; Daturi, M.; Renaud, J.-L. MOF-Assisted Phosphine Free Bifunctional Iron Complex for the Hydrogenation of Carbon Dioxide, Sodium Bicarbonate and Carbonate to Formate. *Chem. Commun.* **2019**, *55*, 4977–4880.
- (24) (a) Knölker, H.-J.; Heber, J.; Mahler, C. H. Transition metal-diene complexes in organic synthesis. Part 14. Regioselective iron-mediated [2+2+1] cycloadditions of alkynes and carbon monoxide: synthesis of substituted cyclopentadienones. *Synlett* **1992**, *1992*, 1002–1004. (b) Knölker, H.-J.; Heber, J. Transition Metal-Diene Complexes in Organic Synthesis, Part 18.1 Iron-Mediated [2+2+1] Cycloadditions of Dienes and Carbon Monoxide: Selective Demetalation Reactions. *Synlett* **1993**, *1993*, 924–926. (c) Knölker, H.-J.; Goesmann, H.; Klaus, R. A Novel Method for the Demetalation of Tricarbonyliron-Diene Complexes by a Photolytically Induced Ligand Exchange Reaction with Acetonitrile. *Angew. Chem. Int. Ed.* **1999**, *38*, 702–705.
- (25) Moulin, S.; Dentel, H.; Pagnoux-Ozherelyeva, A.; Gaillard, S.; Poater, A.; Cavallo, L.; Lohier, J.-F.; Renaud, J.-L. Bifunctional (Cyclopentadienone)Iron-Tricarbonyl Complexes: Synthesis, Computational Studies and Application in Reductive Amination. *Chem.—Eur. J.* **2013**, *19*, 17881–17890.
- (26) (a) Mérel, D. S.; Elie, M.; Lohier, J.-F.; Gaillard, S.; Renaud, J.-L. Bifunctional Iron Complexes: Efficient Catalysts for C=O and C=N Reduction in Water. *ChemCatChem* **2013**, *5*, 2939–2945. (b) Pagnoux-Ozherelyeva, A.; Pannetier, N.; Mbaye, D. M.; Gaillard, S.; Renaud, J.-L. Knölker's Iron Complex: An Efficient In Situ Generated Catalyst for Reductive Amination of Alkyl Aldehydes and Amines. *Angew. Chem.* **2012**, *124*, 5060–5064; *Angew. Chem., Int. Ed.* **2012**, *51*, 4976–4980. (c) Seck, C.; Mbaye, M. D.; Coufourier, S.; Lator, A.; Lohier, J.-F.; Poater, A.; Ward, T. R.; Gaillard, S.; Renaud, J.-L. Alkylation of Ketones Catalyzed by Bifunctional Iron Complexes: From Mechanistic Understanding to Application. *ChemCatChem* **2017**, *9*, 4410–4416.
- (27) Gimferrer, M.; Joly, N.; Escayola, S.; Viñas, E.; Gaillard, S.; Solà, M.; Renaud, J.-L.; Salvador, P.; Poater, A. Knölker Iron Catalysts for Hydrogenation revisited: Non Spectator Solvent and fine-tuning. *Organometallics* **2022**, *41*, 1204–1215.
- (28) Watson, J. D.; Field, L. D.; Ball, G. E. $[\text{Fp}(\text{CH}_4)]^+$, $[\eta^5\text{-CpRu}(\text{CO})_2(\text{CH}_4)]^+$, and $[\eta^5\text{-CpOs}(\text{CO})_2(\text{CH}_4)]^+$: A Complete Set of Group 8 Metal-Methane Complexes. *J. Am. Chem. Soc.* **2022**, *144*, 17622–17629.
- (29) Kim, A. N.; Stoltz, B. M. Recent Advances in Homogeneous Catalysts for the Asymmetric Hydrogenation of Heteroarenes. *ACS Catal.* **2020**, *10*, 13834–13851.
- (30) Tadiello, L.; Gandini, T.; Stadler, B. M.; Tin, S.; Jiao, H.; de Vries, J. G.; Pignataro, L.; Gennari, C. Regiodivergent Reductive Opening of Epoxides by Catalytic Hydrogenation Promoted by a (Cyclopentadienone)iron Complex. *ACS Catal.* **2022**, *12*, 235–246.
- (31) von der Höh, A.; Berkessel, A. Insight into the Mechanism of Dihydrogen-Heterolysis at Cyclopentadienone Iron Complexes and Subsequent C-X Hydrogenation. *ChemCatChem* **2011**, *3*, 861–867.
- (32) Zhang, H.; Chen, D.; Zhang, Y.; Zhang, G.; Liu, J. On the mechanism of carbonyl hydrogenation catalyzed by iron catalyst. *Dalton Trans.* **2010**, *39*, 1972–1978.
- (33) Hackl, L.; Ho, L. P.; Bockhardt, D.; Bannenberg, T.; Tamm, M. Tetraaminocyclopentadienone Iron Complexes as Hydrogenation Catalysts. *Organometallics* **2022**, *41*, 836–851.
- (34) Lu, X.; Cheng, R.; Turner, N.; Liu, Q.; Zhang, M.; Sun, X. High Chemoselectivity of an Advanced Iron Catalyst for the Hydrogenation of Aldehydes with Isolated C = C Bond: A Computational Study. *J. Org. Chem.* **2014**, *79*, 9355–9364.
- (35) Lu, X.; Zhang, Y.; Yun, P.; Zhang, M.; Li, T. The mechanism for the hydrogenation of ketones catalyzed by Knölker's iron-catalyst. *Org. Biomol. Chem.* **2013**, *11*, 5264–5277.
- (36) Lator, A.; Gaillard, S.; Poater, A.; Renaud, J.-L. Well-Defined Phosphine-Free Iron-Catalyzed N-Ethylation and N-Methylation of Amines with Ethanol and Methanol. *Org. Lett.* **2018**, *20*, 5985–5990.
- (37) Bütikofer, A.; Chen, P. Zwitterionic Halido Cyclopentadienone Iron Complexes and Their Catalytic Performance in Hydrogenation Reactions. *Inorg. Chem.* **2023**, *62*, 4188–4196.
- (38) Falivene, L.; Cao, Z.; Petta, A.; Serra, L.; Poater, A.; Oliva, R.; Scarano, V.; Cavallo, L. Towards the online computer-aided design of catalytic pockets. *Nat. Chem.* **2019**, *11*, 872–879.
- (39) (a) Mayer, I. Charge, Bond Order and Valence in the AB Initio SCF Theory. *Chem. Phys. Lett.* **1983**, *97*, 270–274. (b) Mayer, I. Bond Order and Valence: Relations to Mulliken's Population Analysis. *Int. J. Quantum Chem.* **1984**, *26*, 151–154.
- (40) Reed, A. E.; Weinstock, R. B.; Weinhold, F. Natural Population Analysis. *J. Chem. Phys.* **1985**, *83*, 735–746.
- (41) Gonçalves, T. P.; Huang, K.-W. Metal-Ligand Cooperative Reactivity in the (Pseudo)-Dearomatized $\text{PN}_x(\text{P})$ Systems: The Influence of the Zwitterionic Form in Dearomatized Pincer Complexes. *J. Am. Chem. Soc.* **2017**, *139*, 13442–13449.
- (42) Matito, E.; Poater, J.; Duran, M.; Solà, M. An analysis of the changes in aromaticity and planarity along the reaction path of the simplest Diels-Alder reaction. Exploring the validity of different indicators of aromaticity. *J. Mol. Struct. THEOCHEM* **2005**, *727*, 165–171.
- (43) (a) Poater, J.; Gimferrer, M.; Poater, A. Covalent and Ionic Capacity of MOFs To Sorb Small Gas Molecules. *Inorg. Chem.* **2018**, *57*, 6981–6990. (b) Palusiak, M.; Simon, S.; Solà, M. Interplay between intramolecular resonance-assisted hydrogen bonding and local aromaticity. II. 1,3-dihydroxyaryl-2-aldehydes. *J. Org. Chem.* **2009**, *74*, 2059–2066. (c) Richmond, C. J.; Escayola, S.; Poater, A. Axial Ligand effects of Ru-BDA Complexes in the O-O Bond Formation via the I2M Bimolecular Mechanism in Water Oxidation Catalysis. *Eur. J. Inorg. Chem.* **2019**, *2019*, 2101–2108.
- (44) (a) Salvador, P.; Ramos-Córdoba, E. An Approximation to Bader's Topological Atom. *J. Chem. Phys.* **2013**, *139*, 071103. (b) Ramos-Córdoba, E.; Postils, V.; Salvador, P. Oxidation States from Wave Function Analysis. *J. Chem. Theory Comput.* **2015**, *11*, 1501–1508.
- (45) Examples of EOS applications: (a) Gimferrer, M.; Salvador, P.; Poater, A. Computational Monitoring of Oxidation States in Olefin Metathesis. *Organometallics* **2019**, *38*, 4585–4592. (b) Posada-Pérez, S.; Escayola, S.; Poater, J.; Solà, M.; Poater, A. Ni(I)-TPA stabilization by hydrogen bond formation on the second coordination sphere: a DFT characterization. *Dalton Trans.* **2022**, *51*, 12585–12595. (c) Heitkämper, J.; Posada-Pérez, S.; Escayola, S.; Solà, M.; Kästner, J.; Poater, A. A non expected alternative Ni(0) Species in the Ni-Catalytic Aldehyde and Alcohol Arylation Reactions Facilitated by a 1,5-Diaza-3,7-diphosphacyclooctane Ligand. *Chem.—Eur. J.* **2023**, *29*, e202300193.
- (46) Amin, S. R.; Crowe, W. E. Reduction of Imines via Titanium-Catalyzed Hydromagnesation. *Tetrahedron Lett.* **1997**, *38*, 7487–7490.
- (47) Lu, X.; Zhang, Y.; Turner, N.; Zhang, M.; Li, T. Using computational methods to explore improvements to Knölker's iron catalyst. *Org. Biomol. Chem.* **2014**, *12*, 4361–4371.
- (48) Frisch, M. J.; Trucks, G. W.; Schlegel, H. B.; Scuseria, G. E.; Robb, M. A.; Cheeseman, J. R.; Scalmani, G.; Barone, V.; Mennucci, B.; Petersson, G. A.; Nakatsuji, H.; Caricato, M.; Li, X.; Hratchian, H. P.; Izmaylov, A. F.; Bloino, J.; Zheng, G.; Sonnenberg, J. L.; Hada, M.; Ehara, M.; Toyota, K.; Fukuda, R.; Hasegawa, J.; Ishida, M.; Nakajima, T.; Honda, Y.; Kitao, O.; Nakai, H.; Vreven, T.; Montgomery, J. A., Jr.; Peralta, J. E.; Ogliaro, F.; Bearpark, M.; Heyd, J. J.; Brothers, E.; Kudin, K. N.; Staroverov, V. N.; Kobayashi, R.; Normand, J.; Raghavachari, K.; Rendell, A.; Burant, J. C.; Iyengar, S. S.; Tomasi, J.; Cossi, M.; Rega, N.; Millam, J. M.; Klene, M.; Knox, J. E.; Cross, J. B.; Bakken, V.; Adamo, C.; Jaramillo, J.; Gomperts, R.;

Stratmann, R. E.; Yazyev, O.; Austin, A. J.; Cammi, R.; Pomelli, C.; Ochterski, J. W.; Martin, R. L.; Morokuma, K.; Zakrzewski, V. G.; Voth, G. A.; Salvador, P.; Dannenberg, J. J.; Dapprich, S.; Daniels, A. D.; Farkas, Ö.; Foresman, J. B.; Ortiz, J. V.; Cioslowski, J.; Fox, D. J. *Gaussian 09*, rev. E.01; Gaussian, Inc.: Wallingford, CT, 2009.

(49) (a) Becke, A. Density-functional Exchange-Energy Approximation with Correct Asymptotic Behavior. *Phys. Rev. A: At., Mol., Opt. Phys.* **1988**, *38*, 3098–3100. (b) Perdew, J. P. Density-Functional Approximation for the Correlation Energy of the Inhomogeneous Electron Gas. *Phys. Rev. B* **1986**, *33*, 8822–8824.

(50) Schäfer, A.; Huber, C.; Ahlrichs, R. Fully optimized contracted Gaussian basis sets of triple zeta valence quality for atoms Li to Kr. *J. Chem. Phys.* **1994**, *100*, 5829.

(51) (a) Küchle, W.; Dolg, M.; Stoll, H.; Preuss, H. Energy-adjusted pseudopotentials for the actinides. Parameter sets and test calculations for thorium and thorium monoxide. *J. Chem. Phys.* **1994**, *100*, 7535–7542. (b) Leininger, T.; Nicklass, A.; Stoll, H.; Dolg, M.; Schwerdtfeger, P. The accuracy of the pseudopotential approximation. II. A comparison of various core sizes for indium pseudopotentials in calculations for spectroscopic constants of InH, InF, and InCl. *J. Chem. Phys.* **1996**, *105*, 1052–1059.

(52) Zhao, Y.; Truhlar, D. G. The M06 suite of density functionals for main group thermochemistry, thermochemical kinetics, non-covalent interactions, excited states, and transition elements: two new functionals and systematic testing of four M06-class functionals and 12 other functionals. *Theor. Chem. Acc.* **2008**, *120*, 215–241.

(53) Weigend, F.; Ahlrichs, R. Balanced basis sets of split valence, triple zeta valence and quadruple zeta valence quality for H to Rn: Design and assessment of accuracy. *Phys. Chem. Chem. Phys.* **2005**, *7*, 3297–3305.

(54) Barone, V.; Cossi, M. Quantum Calculation of Molecular Energies and Energy Gradients in Solution by a Conductor Solvent Model. *J. Phys. Chem. A* **1998**, *102*, 1995–2001.

(55) Tomasi, J.; Persico, M. Molecular Interactions in Solution: An Overview of Methods Based on Continuous Distributions of the Solvent. *Chem. Rev.* **1994**, *94*, 2027–2094.